Micro heterogeneous fatigue behavior of duplex stainless steel during cyclic loading

G. Chai[1,3a]*, R. Lillbacka[2b], and R. Lin Peng[3c]

[1]Sandvik Materials Technology, R&D Centre, 811 81 Sandviken, Sweden

[2]FSDYNAMIC, Mölndalsvägen 24 , 412 63 Göteborg , Sweden

[3]Dept of Mechanical Engineering, Linköping University, S-581 83 Linköping, Sweden

[a]guocai.chai@sandvik.com, [b]robert.lillbacka@fsdynamics.se, [c]Ru.Peng@liu.se,

Keywords: Fatigue damage, Fatigue crack initiation, Low cycle fatigue, Multi-scale material modeling, Duplex stainless steels.

Abstract. Two phase metals can suffer from non-uniform load sharing between the phases or stress heterogeneity on the micro-scale, elastic/plastic anisotropy and other mechanical interactions on the scale of grain size during cyclic loading. These effects strongly influence the fatigue damage and crack initiation behaviour of the two phase metals. In this paper, the fatigue damage and crack initiation behaviours of two austenitic-ferritic duplex stainless steels, UNS S32750 and UNS S32906, have been studied by both experimental investigations such as low cycle fatigue tests, SEM and TEM study, and X-ray and neutron diffraction and simulation using multi-scale material modelling. It has been found that the material damage and crack initiation in these two duplex stainless steels during cyclic loading occur mainly in the ferritic phase that is the weakest phase if the deformation hardening is considered.

Introduction

Multiphase materials due to their microstructures and excellent properties are becoming more attractive for both engineering applications and academic interests. Duplex stainless steels (DSS) are a group of steels that consist of approximately equal volume of austenite and ferrite. Due to a good combination of excellent corrosion resistance and high mechanical properties, they are increasingly employed in various industries [1], and their fatigue behaviours have also been widely studied during last decades [2-5].

Much research work has been done to understand the cyclic deformation mechanisms and the low-cycle fatigue damage mechanisms of DSS [3-5]. It has been found that LCF behaviour of DSS can vary with the alloys and the range of applied plastic strains [2-5]. These studies, including the hardening and softening mechanisms, are mainly focused on the mechanical behavior of DSS under uni- and multi-axial cyclic loadings and on the macro scales. In the work by Llanes et. al. [4] it was observed that although the plastic deformation in SAF 2507 starts in the austenite phase, hardness measureed after cyclic loading shows that austenite is the harder one of the two phases. It seems difficult to provide a full explanation to the damage mechanisms unless the meso–micro scale elasto-plastic deformation mechanisms are studied [12].

Duplex stainless steels have two phases with different mechanical and physical properties such as

modulus of elasticity, yield strength and deformation hardening rate, and therefore exhibit micro deformation heterogeneity [6-13]. As a result, both stress and strain are not uniformly distributed at the phases and the actual load sharing on the microscopic scale is dependent on the property mismatch and microstructural features. It is believed that the difference in the elasto-plastic properties between the phases and the coupling effect, i.e., the load and strain sharing between the phases, is largely responsible for the varying elasto-plastic deformation mechanisms with varying plastic strain ranges in DSSs [8]. The phase-specific stresses, i.e., the total stresses that the constituent phases are subjected to is the sum of macrostresses, corresponding directly to the applied stresses, and microstresses due to micromechanical responses. The importance of micromechanical interactions under mechanical load has been recognized [8, 9].

Recently, the micro yielding and damage behavior of the austenitic and ferritic phases in duplex stainless steels during cyclic loading have been studied by in-situ X-ray and neutron diffraction and multiscale modelling [8-13]. The influence of composition, microstructure and loading on the micro yielding and damage behavior of the austenitic and ferritic phases and fracture behavior of DSS have been investigated. This paper provides a review on the methods and the investigations that have been performed with regards to load partitioning and micro cyclic yielding in several super duplex stainless steels.

Materials and experimental

Two commercial DSS, UNS S32750 and UNS S32906, were used in this study. As shown in Table I, UNS S32906 containing higher amounts of Cr and N has a much higher hardness in the austenite. However, UNS S32750 containing a higher amount of Mo shows a higher hardness in the ferrite.

Table I. Nominal compositions (wt%) and mechanical properties of the materials used

Materials	Marks	C	Si	Mn	Cr	Ni	Mo	N	Hv_0,1	
									α	γ
UNS S32750	2507AD	0,03	0,8	1,2	25	7	4	0,3	286	272
UNS S32906	2906AD	0,03	0,5	1,2	29	6	2	0,4	265	298

The low cycle fatigue tests were performed under total strain control condition using a computer controlled servo-hydraulic 100 kN Instron machine at room temperature. The strain was measured using an extensometer with a gauge length of 25mm on round specimens with a diameter of 12mm. A symmetric push-pull mode with a sinusoidal waveform and a cyclic strain rate of $3 \cdot 10^{-5}$/s were applied. The tests were stopped when 20% reduction of the stress amplitude was obtained.

In order to investigate the elasto-plastic deformation mechanism, the dislocation structures were studied using a Jeol 2000-FX analytical transmission electron microscope (TEM/STEM) operating at 200 kV. The slip band localization was investigated using a scanning electron microscopy (SEM). The micro stresses in the austenitic and ferritic phases were measured by in-situ X-ray diffraction and off-situ neutron diffraction. For the neutron diffraction, 10 mm long specimens in as-received condition as well as after cyclic unloading were prepared. A double focusing Si 331 monochromator was used to provide a monochromatic neutron beam with a nominal wavelength of 1.7 Å. The elastic strain measurements were carried out, from which the stresses were derived. For X-ray diffraction, a modified Siemens X-ray diffracometer of ω-type with Cr-Kα radiation was used. A compact tensile test rig was mounted on the X-ray diffractometer to provide uniaxial tensile load during diffraction measurement. The applied stresses were controlled with a 10 kN load-cell and the macroscopic strains were recorded via two strain gauges, one next to the X-ray irradiated area on the front side and the other on the backside of the tensile specimen. The stresses were calculated using the $\sin^2\Psi$-method.

Multi-scale material modeling

In recent years, multi-scale material modelling has gained much interest from the researchers in the field of material mechanics. This type of modelling offers the possibility to study the behaviour of individual phases, individual grains and load sharing between the phases in multi-phase materials. The basic idea in multi-scale material modelling is that the *a priori* homogenized macro- scale material model is replaced by the homogenized response of a representative volume element (RVE), a generation of a numerical grain structure from a physical grain structure using RVE (Fig. 1) [10, 12].

Multi-scale material modelling uses micro-scale crystal plasticity and continuum models [10]. The basic idea is to perform numerical homogenization of the material behaviour in a representative volume element (RVE) using the finite element method. Hence, the given macro-scale strain from the experimental LCF tests are applied as boundary conditions on the RVE and the macro-scale Cauchy stress is calculated as the volume average, over the RVE, of the corresponding micro-scale Cauchy stress

$$\bar{\boldsymbol{\sigma}} = \frac{1}{\mathrm{V}}\int_{\Omega} \boldsymbol{\sigma}\mathrm{dV}\,. \tag{1}$$

where the micro-scale Cauchy stress is obtained from the crystal plasticity model described below. The RVE, which mimics the austenitic-ferritic duplex stainless steel is generated using a Voronoi polygonization algorithm, and it is shown in Figure 1b. Crystallographic directions are also randomly assigned to the grains since these are needed in the crystal plasticity model which represents the material behavior in a material point inside one grain. The crystal plasticity model is thoroughly discussed in [10], here we shall just give the main equations. The yield functions are stated in terms of the shear (Schmid) stress in the slip systems

$$\varphi_\alpha = |\tau_\alpha| - \left(\sigma_\alpha^{\mathrm{y}} + \kappa_\alpha\right). \tag{2}$$

where $\sigma_\alpha^{\mathrm{y}}$ is the initial yield stress and κ_α is the hardening stress which follows the evolution law

$$\dot{\kappa}_\alpha = \sum_\beta \left(q + (1-q)\delta_{\alpha\beta}\right) h_\beta\left(A_\beta\right)\dot{\gamma}_\beta \;\text{ with }\; \beta = 1,2,\ldots,\mathrm{Nr.slip}\,. \tag{3}$$

Here, q is a parameter which determines the amount of cross hardening and $\delta_{\alpha\beta}$ is the Kronecker delta. The hardening function $h_\beta\left(A_\beta\right)$ was suggested [10] but here it has been modified by the authors to account for cyclic softening.

$$h_\alpha\left(A_\alpha\right) = h_0 + \left(h_\infty - h_0\right)\left(1 - \mathrm{e}^{\left(-\xi \mathrm{A}_\alpha\right)}\right) - h_{\mathrm{s}}\left(1 - \mathrm{e}^{\left(-\xi_{\mathrm{s}} \mathrm{A}_\alpha\right)}\right) \;\text{ with }\; \dot{A}_\alpha = \sum_\beta \left(q + (1-q)\delta_{\alpha\beta}\right)\dot{\gamma}_\beta \tag{4}$$

hence, h_0 is the initial hardening modulus, h_∞ determines the saturation of the hardening and h_{s} determines the softening of the hardening modulus, ξ and ξ_{s} determines the rate at which the hardening and softening saturates respectively. For the evolution of the plastic slip a viscoplastic format of Perzyna type is adopted.

$$\dot{\gamma}_\alpha\left(\varphi_\alpha\right) = \frac{1}{t_*}\left(\left(\frac{\langle\varphi_\alpha\rangle}{\sigma_\alpha^{\mathrm{y}} + \kappa_\alpha} + 1\right)^n - 1\right) \;\text{ with }\; \langle x\rangle \overset{\mathrm{def}}{=} \frac{1}{2}\left(x + |x|\right). \tag{5}$$

where, t_* is the relaxation time and n is the creep exponent. Note that t_* is only included for numerical relaxation and that it is chosen small enough so that plastic response is obtained.

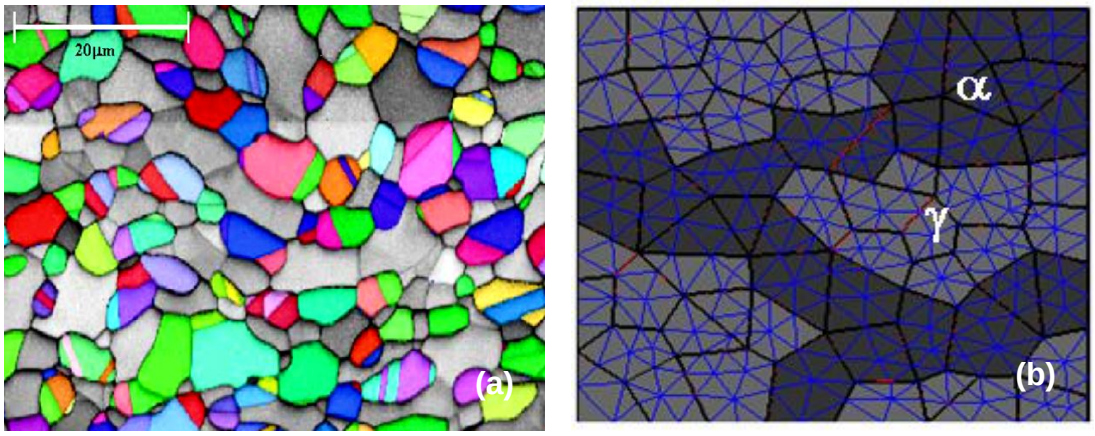

Fig. 1. (a). Grain structure of duplex stainless steel, grey: ferritic phase; color: austenitic phase, (b). Numerical grain structure generated by using Representative Volume Element (RVE) byVoronoi polygonization algorithms, α: ferritic phase; γ: austenitic phase.

Results and discussion

Micro yielding behaviour in duplex stainless steels. The micro yielding behaviour of the individual phases in two phase alloys can be described by the phase-specific stress versus the macroscopic strain curves. Fig. 2 shows the micro deformation behaviour and load sharing between the austenitic and ferritic phases measured by in-situ X-ray diffraction method in 2507AD (Fig. 2a) and micro stresses versus strain from the multiscale simulation (Fig. 2b). It shows that the austenitic phase is initially a soft phase. With straining, yielding in the austenitic phase starts to occur at an early stage of loading. Since the deformation hardening rate is higher in the austenite than in the ferrite, the austenitic phase becomes then a stronger phase with further straining. This is clearly shown in Fig. 2b. This result is comparable to the micro hardness measurements in the same material [12]. Fig. 1a also shows the change of residual micro stresses in the individual phases after either macroscopic elastic or plastic loading. The above results conclude that a stronger or weaker phase in a duplex stainless steel is relative, depending on the composition and plastic deformation in the material.

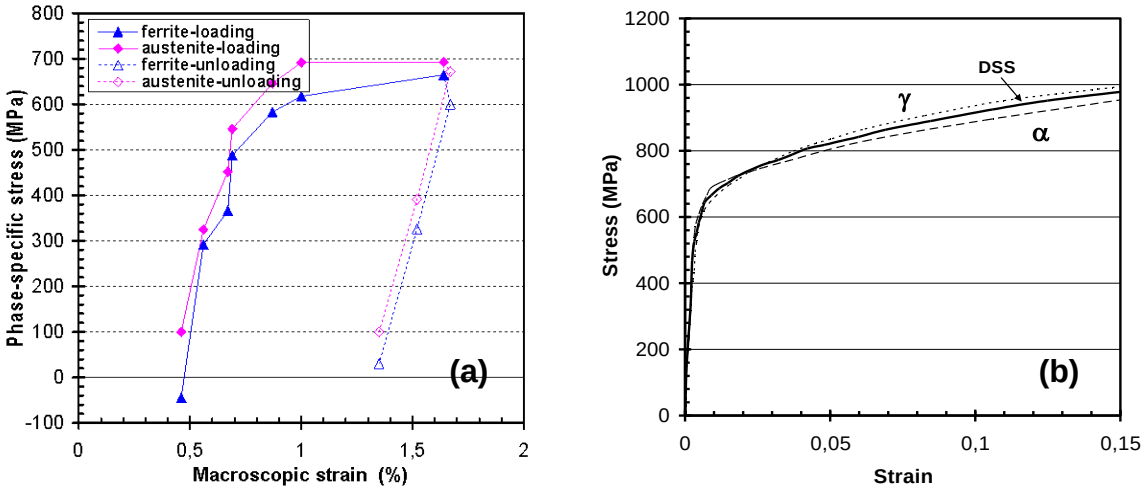

Fig. 2. Phase-specific stress or micro stress versus strain in UNS S32750 material.

Low cycle fatigue damage and phase interactions. In order to investigate the damage process, a low cycle fatigue test with a strain amplitude of 0.5% was interrupted after reaching 1, 10, 100 and 3000 cycles, respectively, to obtain specimens for the neutron diffraction measurements. These represent three distinct stages: initial hardening, softening and saturation before fracture occurs (Figure 3a).

The diffraction peak width averaged over all the measurement directions of respective *hkl* planes is plotted as Full Width at Half Maximum intensity (FWHM) in Fig. 3b for UNS S32750. For a given diffraction set-up and material condition, any variation of the peak width indicates changes in the inhomogeneous elastic strains within the diffraction volume. In this case, the variation of FWHM observed in Fig. 3b can be interpreted as the influence of cyclic loading on the dislocation density or residual stress gradient. The obvious decrease of peak width of γ–(220), γ– (311), α–(211) and α-(200) after the first load cycle could probably be explained by a large macroscopic stress gradient before fatigue loading, which has been reduced by the first load cycle. With continued loading from 1 to 100 cycles, the FWHM of the austenitic planes increases slightly, implying little changes in the dislocation density. A more significant increase is found above 100 cycles. On the other hand, the FWHM of the ferritic planes continues to decrease and an obvious increase is only found after loading to 10 cycles for the (211) plane and 100 cycles for the (200) plane. Furthermore, loading above 100 cycles causes a more significant broadening of the ferritic-(211) peak than the austentic peaks. These observations indicate that very small damage can occur in the austenitic phase in the beginning of the cyclic loading. After 10 cycles, the damage in the ferrite starts to occur and continues. After about 100 cycles, the damage in the austenitic phase can also continue. The results also indicate that the damage in ferritic phase is higher than that in the austenitic phase after 3000 cycles.

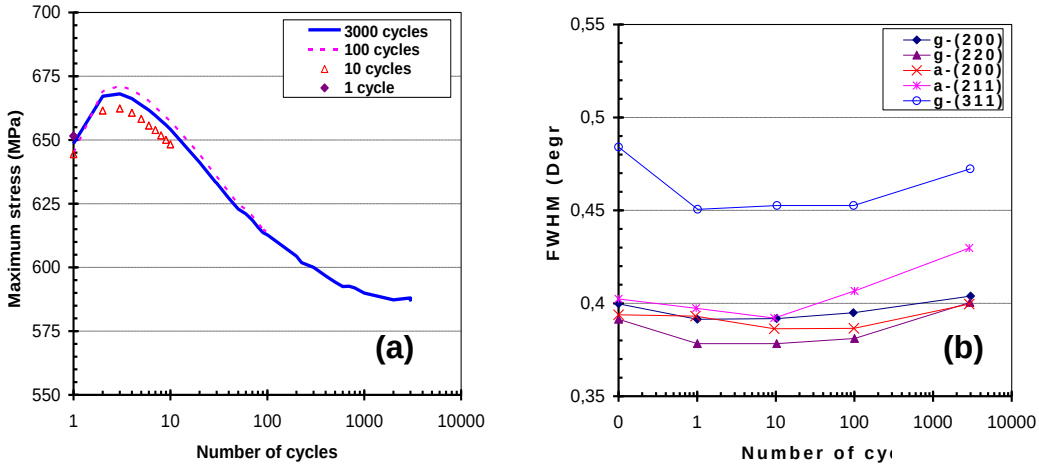

Fig. 3. Diffraction peak (FWHM), averaged over all the measurement directions (g=γ, a=α).

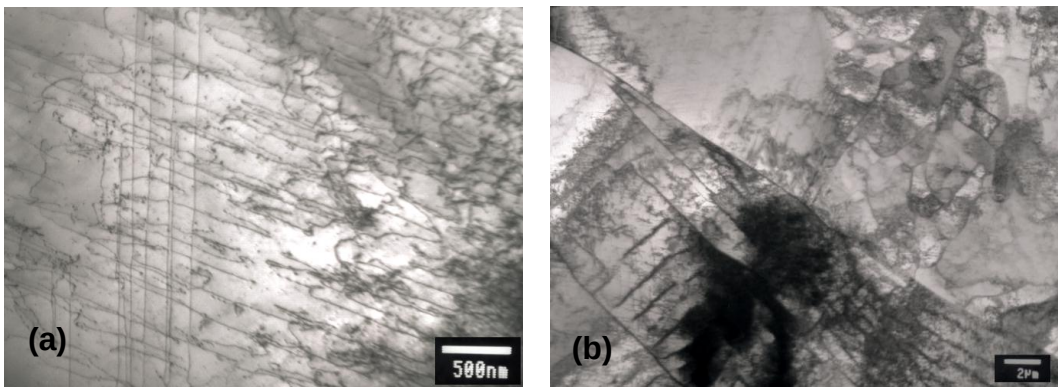

Fig. 4. TEM images show dislocation structures developed in SAF 2507 DSS material, (a). Planar array dislocations in the austenite, (b). Channel dislocations in the ferrite.

To verify the above observation, the dislocation substructure was analysed using TEM. The results show that the austenitic phase has mainly a planar array dislocation structure. The dislocation density increases with number of cycles, but the increase rate is relatively low (Figure 4a). Different from the austenitic phase, the dislocation structures in the ferritic phase change with number of cycles. The dislocation structures such as thin dense dislocation walls, long straight dislocations, loops and debris and channel dislocation have developed with increasing number of cycles (Figure 4b). SEM investigation shows that the fatigue pre-initiation damage has occurred in both phases (Figure 6a), but mainly in the ferritic phase.

The above phenomenon was also simulated using multiscale modelling with two DSS materials. Fig. 5 shows the simulated hardening and softening processes occurring in the austenitic and ferritic phases in these two materials. They behave differently. The ferritic phase has a shorter cyclic hardening period and lower hardening rate comparing with the austenitic phase. Another interesting phenomenon is that the softening occurs more quickly in the ferritic phase than in the austenitic phase. The hardening and softening behaviour of the individual phases in different steel grades are also different. In 2507AD, the austenitic phase is initially the soft phase and becomes the stronger phase after two loading cycles. For 2906AD, the austenitic phase is always the stronger phase during the whole cyclic loading process**.** As shown in Table I, 2906AD has a higher nitrogen content. Since nitrogen mainly concentrates in the austenite, the austenite remains a stronger phase during deformation process [11], which is different from 2507AD (Figure 2).

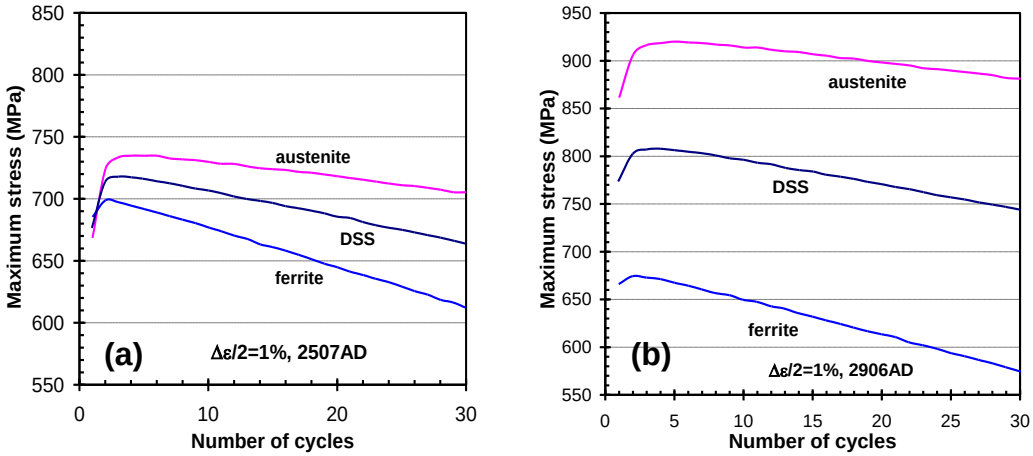

Fig. 5. Simulated cyclic stress response curves for two duplex stainless steels (UNS S32750 and UNS S32906).

Damage in material usually means permanent sub- and microstructural changes (strain localization) and creation of microscopic cracks. Here the micro damage is defined as the formation of slip bands in the individual phases. Figure 6 show the micro damage behaviour (accumulated effective plastic slips) in SAF 2507 and SAF 2906 using multiscale material modelling. More red color represents the areas with a higher amount of plastic slips. For 2507AD, damage (accumulated slip bands) can be seen in both austenitic and ferritic phase, but mainly in the ferritic phase. For 2906AD, the damage is mainly in the ferritic phase. These results are in good agreement with the experimental observations (Fig. 3 and 6c and d). From the above discussions, it can be concluded that damage and crack initiation in a two phase alloy depend on not only the initial strength of the individual phases, but also their deformation hardening behaviour.

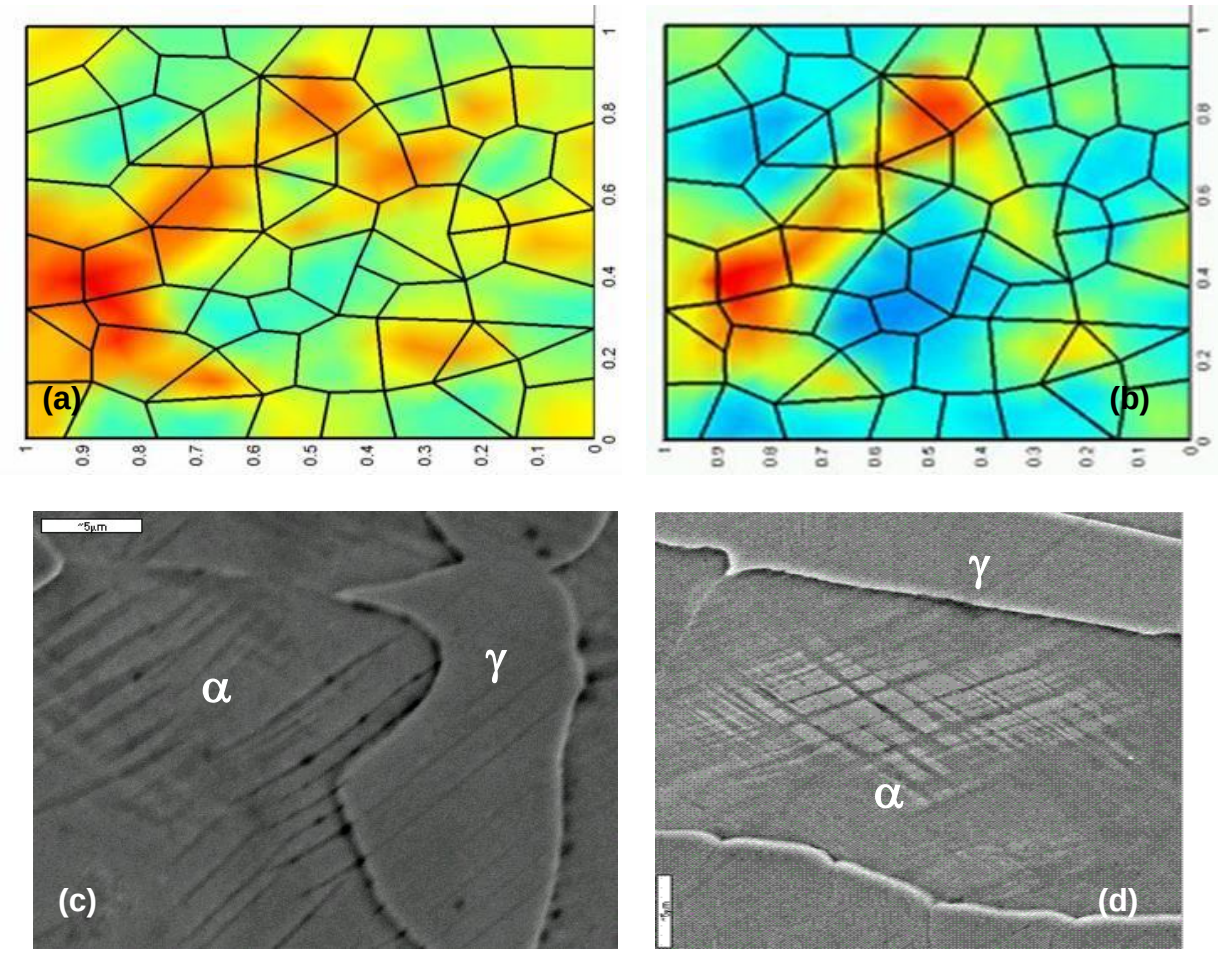

Figure 6. Micro damage in the austenitic and ferritic phases of two duplex stainless steels by cyclic loading with a strain amplitude of 1% using multiscale material modelling (Fig. 6a (2507AD) and Fig 6b (2906AD)), and low cycle fatigue tests (Fig. 6c (2507AD) and Fig. 6d (2906AD)).

Conclusions

In this review, micro yielding and damage (formation of slip band) behaviour in two ferritic-austenitic duplex stainless steels, UNS S32750 and UNS S32906, has been discussed, which leads to the following conclusions:

The deformation behaviour in an individual phase in a multiphase material depends strongly on the composition and deformation condition. For UNS S32750, the austenitic phase yields first even under a macroscopic elastic loading, but can become stronger than the ferritic phase after a large plastic deformation. For UNS S32906, the austenitic phase remains the stronger phase during the whole fatigue process.

Damage and crack initiation in a two phase alloy depend on not only the initial strength of the individual phases, but also their cyclic deformation hardening behaviour. The weaker phase after cyclic loading becomes damaged and hence exhibits crack initiation first.

Acknowledgements

This review paper is published by permission of Sandvik Materials Technology. The authors are also indebted to the co-authors in the reference list for their contribution and collaborations.

References

[1] J. O. Nilsson: Mater. Sci. Technol. No. 8 (1992), p. 685

[2] T. Magnin and J. M. Lardon: Mater. Sci. Eng. 104 (1988), p. 21

[3] S. Degallaix, A. Seddouki, G. Degallaix, T. Kruml and J. Polák: Fatigue Fract. Engng. Mater. Struct. 18 (1995), p. 65

[4] L. Llanes, A. Mateo, P. Villechaise, J. Méndez and M. Anglada. Inter. J. Fatigue, 21 (1999), p.119

[5] J-B. Vogt, K. Massol and J. Foct: Inter. J. Fatigue, 24(6) (2002), p. 627

[6] J.J. Moverare: in *Microstresses and anisotropic mechanical behaviour of duplex stainless steels*, Ph D thesis, (2001), Linköping University, Sweden.

[7] R. Lin Peng, G. Chai, N. Jia, Y. D. Wang and S. Johansson: Fat. & Fract. of Engng. Mat. & Struct., 31(10): (2008), p. 892

[8] N. Jia, R. Lin Peng, Y. D. Wang, G. C. Chai, S. Johansson, G. Wang and P. K. Liaw: ACTA Materialia, 54 (2006) p. 3907

[9] R. Lin Peng, J. Gibmeier, S. Eulert, S. Johansson and G. C. Chai: Materials Science Forum, 524-525 (2006), p. 847

[10] R. Lillbacka: in *On the multiscale modelling of duplex stainless steel*, Ph D thesis, (2007), Chalmers university of technology.

[11] G. Chai, R. Lillbacka and P. Liu: *Damage and crack initiation behaviour of a duplex stainless steel during cyclic loading*, MRS fall meeting, (2005), .Boston.

[12] R. Lillbacka, G. Chai, M. Ekh, P. Liu, E. Johnson and K. Runesson: Acta Materialia, 55 (2007), p. 5359

[13] G. Chai, and R. Lillbacka: Key Engineering Materials, 324-325 (2006), p. 1117